https://doi.org/10.3311/PPci.38403

Periodica Polytechnica Civil Engineering

Numerical Analysis of Temperature Stress Generated by Hydration Heat in Massive Concrete Pier

Junlong Zhou[1], Xiaopeng Li[1], Zihao Wang[2], Yuquan Wang[3], Chuan Yan[4], Hexin Jin[1*]

[1] China Construction Sixth Engineering Bureau Co., Ltd., No. 217 Bawei Road, Hedong District, 300171 Tianjin, China
[2] China Railway Taiyuan Group Co., Ltd., No. 202 Jianshe North Road, Xinghualing District, 030001 Taiyuan, China
[3] China Railway Design Group Co., Ltd., No. 109 Dongqi Road, Dongli District, 300171 Tianjin, China
[4] Central Research Institute of Building and Construction Co., Ltd, No. 30, North Third Ring East Road, 100082 Beijing, China
[*] Corresponding author, e-mail: jinhexin@cscec.com

Received: 25 September 2024, Accepted: 18 December 2024, Published online: 22 January 2025

Abstract

Thermal crack induced by the hydration heat of massive concrete is the main problem that needs to be strictly controlled during the pouring process of concrete. In this study, the hydration heat of massive concrete pier and its influencing factors are studied numerically. The stress of massive concrete pier caused by the hydration heat of concrete is analytically derived. The influences of adiabatic temperature rise, ambient temperature and convection coefficient between the pier outer surface and environment on the temperature and stress of pier are studied. The results show that the peak values of temperature and stress of the pier increase with the increase of the maximum adiabatic temperature rise, the reaction rate coefficient and the ambient temperature. The peak value of stress reduces with the decrease of convection coefficient because the heat dissipation and the temperature change on the cross-section of the pier are reduced.

Keywords

thermal stress, hydration heat, massive concrete pier, early cracks, analytical method

1 Introduction

Massive concrete structure is extensively used in engineering project. During the early stage of concrete curing, the heat generated by hydration can adversely affect the early crack resistance of concrete, potentially resulting in early cracking due to material properties and complex construction conditions [1]. These cracks may reduce the safety and durability of the structure. Because of the low thermal conductivity of concrete, hydration heat accumulates within the newly poured structure, causing the internal temperature to rise continuously while the surface temperature remains close to the ambient temperature. The temperature gradient distribution may lead to cracking in the concrete structure [2–5].

For complex structure, the temperature of hydration heat and stress induced by thermal expansion are always difficult to derive analytically [6, 7]. The generation of hydration heat and cracking in concrete involves numerous complex factors, such as temperature changes, material properties, construction conditions, and curing methods. As a mixture, concrete exhibits significant differences in its internal structure and properties at different stages, especially during the early-age period, where properties such as strength, elastic modulus, and shrinkage vary greatly [8, 9]. Zienkiewicz demonstrated the promotion of relaxation analysis method on temperature stress problem in concrete structure, and derived the temperature stress induced by the hydration heat in massive concrete structure [10]. However, the analytical solution was only an approximate result, and the validity of this result was based on some rigorous assumptions. Considering the influence of temperature on the creep characteristics and hydration reaction rate of early-age concrete, Zhang et al. proposed a semi-analytical iterative method for solving temperature, stress and concrete crack propagation of early-age concrete [11]. Wang et al. proposed a temperature field prediction model based on artificial neural network algorithm for the transient analysis of temperature field in massive concrete [12]. Analytical methods often rely on certain assumptions and simplified conditions, which may deviate significantly from actual situations, leading to inaccurate results.

Cite this article as: Zhou, J., Li, X., Wang, Z., Wang, Y., Yan, C., Jin, H. "Numerical Analysis of Temperature Stress Generated by Hydration Heat in Massive Concrete Pier", Periodica Polytechnica Civil Engineering, 2025. https://doi.org/10.3311/PPci.38403

The finite element method is widely used to analyze the stress caused by hydration heat of concrete [13, 14]. In 1968, Wilson developed the first finite element simulation program to estimate the hydration heat of the Hoover Dam [15]. Nobuhiro et al. predicted the cracks in massive concrete via the softwares ADINAT and ADINA [16]. Barrett et al. numerically evaluated the temperature stress and cracking issue in dam based on the concrete cracking model via a 3D numerical software [17]. Emborg et al. investigated the effects of steel reinforcement, thermal performance and mechanical properties of early age concrete on the concrete cracking, and the results showed that only considering the early distribution of the temperature field within the structure is insufficient to control the temperature stress and crack in the structure [18]. The finite element method for solving and calculating the hydration heat of large volume concrete has the characteristics of high calculation accuracy and wide applicability of structural forms. However, the finite element method also has the disadvantages of requiring a large amount of memory for calculation, complex calculation process, and high requirements for computing equipment.

In this study, a 3D numerical model of massive concrete pier is established via the commercial software Midas FEA NX [19]. An analytical method is proposed to calculate the thermal stress of massive concrete pier. The influences of adiabatic temperature rise, ambient temperature and convection coefficient on the temperature and thermal stress field of pier are studied. Fig. 1 is the logical flowchart of this study.

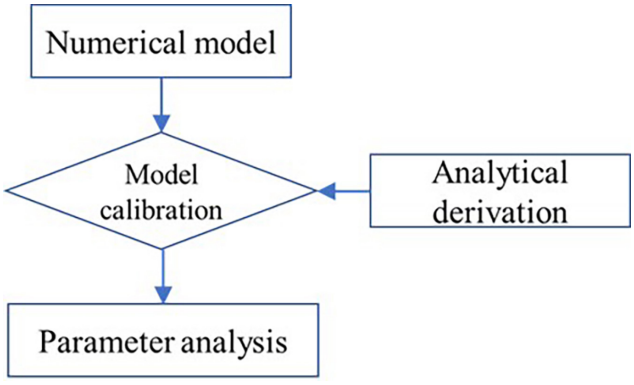

Fig. 1 Logical flowchart of this study

2 Temperature and stress field of concrete pier induced by hydration heat

2.1 Numerical model of concrete pier

In order to study the thermal stress caused by the hydration heat of concrete in pier, a numerical model of concrete pier as shown in Fig. 2 is established via the software MIDAS FEA NX. The concrete pier is a cylindrical pier with a radius of 1 m and a height of 20 m. Due to the symmetry of the pier, a quarter of the pier is taken as the research object, and symmetrical boundaries are applied to the pier. Fixed end boundary is applied at the bottom of the pier. In this study, the influence of steel reinforcement on the hydration heat of concrete is ignored. Therefore, steel reinforcement is not established in the model. The ambient temperature and the fixed end temperature of the model are both set to 20 °C [20].

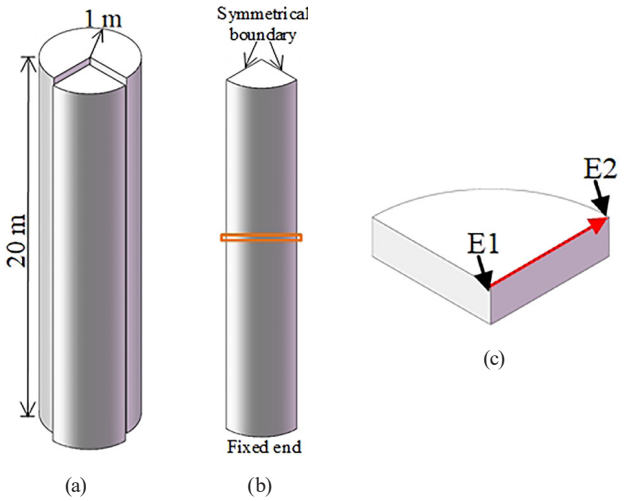

Fig. 2 Numerical model of cylindrical pier (a) cylindrical pier; (b) a quarter of cylindrical pier; (c) enlarged cylindrical pier

Under adiabatic heating condition, the hydration heat of concrete is completely used to increase the temperature of pier. The adiabatic temperature rise of concrete can be predicted based on the [21–23].

$$T(t)=\frac{m_c Q}{\kappa\rho}(1-e^{-\eta t}), \tag{1}$$

where m_c is the cement usage per cubic meter of concrete, Q is the hydration heat per kilogram of cement, and the value are given in Table 1. κ is the specific heat of concrete, η is the reaction rate coefficient. $m_c Q/\kappa\rho$ is the maximum adiabatic temperature rise of concrete pier induced by concrete hydration heat.

The surface of pier directly contact with air, which leads to heat exchange between pier and air. The heat exchange

Table 1 Hydration heat per kilogram of cement (kJ/Kg) [24]

Type	No. 225	No. 275	No. 325	No. 425	No. 525
Ordinary Portland cement	201	243	289	377	461
Slag Portland cement	188	205	247	335	

is characterized by the convective heat transfer coefficient, and is calculated by [25].

$$\beta = 18.46 + 17.36v^{0.883}, \tag{2}$$

where v is the wind speed.

Considering the effect of thermal insulation measure on the hydration heat of concrete, the equivalent convective heat transfer coefficient, as given in Eq. (3), is used [23, 26].

$$\beta_{eq} = \frac{1}{\sum h_i/\lambda_i + 1/\beta}, \tag{3}$$

where λ_i and h_i are the conductivity factor and thickness of the i-th layer of the insulation material, β is the convective heat transfer coefficient between outermost insulation layer and the surrounding environment.

The concrete in this model is assumed to be isotropic linear elastic state. The thermodynamic parameters of concrete do not change with time, concrete strength and temperature. The concrete pier model is simulated by hexahedral solid element. The physical and thermal parameters of concrete are given in Tables 2 and 3, respectively.

2.2 Mesh size sensitivity analysis

In the finite element analysis, the mesh size affects computational time and accuracy. To optimize the effects of these two factors, a mesh sensitivity test is carried out. Three mesh sizes, namely, 5 cm, 10 cm and 15 cm, are considered. Fig. 3 illustrates the stress time history on the middle section of the pier outer edge corresponding to different mesh sizes. It can be seen that 10 cm mesh size yields almost the same prediction as that with the mesh size 5 cm whereas the simulations with the larger element size of 15 cm give different predictions. Considering the accuracy and the efficiency for simulation, the finite element model with mesh size of 10 cm is used in this study.

Table 2 Physical parameters of concrete [27, 28]

Compressive strength (MPa)	Elastic modulus (GPa)	Density (kg/m^3)	Poisson's ratio
40	42	2550	0.2

Table 3 Thermal parameters of concrete [29]

Thermal expansion coefficient (1/°C)	Conductivity factor (kJ/m · h · °C)	Specific heat (kJ/ kg · °C)	Maximum adiabatic temperature rise (°C)	Reaction rate coefficient (1/h)
$1 \cdot 10^{-5}$	9.2988	0.918	85	0.015

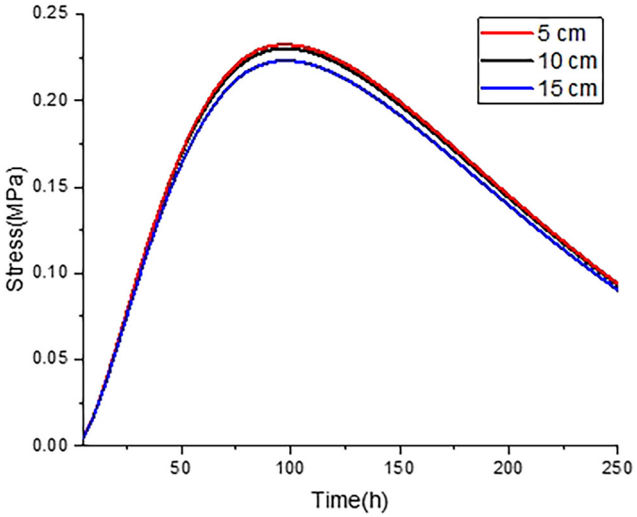

Fig. 3 Influence of mesh size on the stress time history on the middle section of the pier outer edge

2.3 Analytical derivation of temperature and stress fields of pier

Due to the large aspect ratio of the cylindrical pier, the influence of the fixed and free ends of the pier is ignored, and the hydration heat problem of the pier in this study is simplified into a plane strain problem [22].

To solve the stress and displacement induced by concrete hydration heat in pier, the displacement potential ϕ is introduced, and the displacement potential satisfies the following condition.

$$\nabla^2\phi = \frac{1+\mu}{1-\mu}\alpha T, \tag{4}$$

where μ is the poisson's ratio of concrete, α is the coefficient of linear thermal expansion, T is the temperature of concrete, and $\nabla^2 = \frac{\partial^2}{\partial r^2} + \frac{1}{r}\frac{\partial}{\partial R} + \frac{1}{r^2}\frac{\partial^2}{\partial \theta}$.

The displacement specific solutions can be calculated by:

$$u_{r1} = \frac{\partial \phi}{\partial r}, \tag{5}$$

$$u_{\theta 1} = \frac{\partial \phi}{\partial \theta}, \tag{6}$$

where r and θ are the radial and tangential polar coordinates of pier, respectively.

Due to the symmetry of the cylindrical pier in this study, the displacement potential function is only related to the radius r. By solving Eq. (4), the displacement potential function can be obtained as:

$$\phi(r)=\frac{1+\mu}{1-\mu}\alpha\int\frac{1}{r}\int T(r)rdr^2+\frac{1+\mu}{1-\mu}\alpha A\ln r+B\,, \tag{7}$$

where A and B are constants.

The stress and displacement corresponding to the displacement potential are:

$$\sigma_{r1}=\frac{E\alpha}{(1-\mu)r^2}\left(\int T(r)rdr+A\right), \tag{8}$$

$$\sigma_{\theta1}=\frac{E\alpha}{(1-\mu)r^2}\left(\int T(r)rdr+A-T(r)r^2\right), \tag{9}$$

$$\tau_{r\theta1}=0\,, \tag{10}$$

$$u_{r1}=\frac{(1+\mu)\alpha}{(1-\mu)r}\left(\int T(r)rdr+A\right), \tag{11}$$

where E is the elastic modulus of concrete.

To obtain the stress supplementary solution, a stress function that satisfies the compatibility equation is introduced. The compatibility equation is:

$$\left(\frac{\partial^2}{\partial r^2}+\frac{1}{r}\frac{\partial}{\partial r}+\frac{1}{r^2}\frac{\partial^2}{\partial\theta^2}\right)^2\psi=0\cdot \tag{12}$$

The stress function is:

$$\psi=\frac{C}{2}r^2\,, \tag{13}$$

where C is constant.

The stress supplementary solutions are:

$$\sigma_{r2}=\frac{1}{r}\frac{\partial\psi}{\partial r}+\frac{1}{r^2}\frac{\partial^2\psi}{\partial\theta^2}=C\,, \tag{14}$$

$$\sigma_{\theta2}=\frac{\partial^2\psi}{\partial r^2}=C\,, \tag{15}$$

$$\tau_{r\theta2}=\frac{\partial\psi}{\partial r}\left(\frac{1}{r}\frac{\partial\psi}{\partial\theta}\right)=0\cdot \tag{16}$$

The displacement supplementary solution is obtained as:

$$u_{r2}=rC\frac{(1-2\mu)(1+\mu)}{E}\,. \tag{17}$$

The stress and displacement solutions are:

$$\sigma_r=\sigma_{r1}+\sigma_{r2}=-\frac{E\alpha}{(1-\mu)r^2}\left(\int T(r)rdr+A\right)+C\,, \tag{18}$$

$$\sigma_\theta=\sigma_{\theta1}+\sigma_{\theta2}=-\frac{E\alpha}{(1-\mu)r^2}\left(\int T(r)rdr+A-T(r)r^2\right)+C, \tag{19}$$

$$\tau_{r\theta}=\tau_{r\theta1}+\tau_{r\theta2}=0\,, \tag{20}$$

$$u_r=u_{r1}+u_{r2}=\frac{(1+\mu)\alpha}{(1-\mu)r}\left(\int T(r)rdr+A\right)+rC\frac{(1-2\mu)(1+\mu)}{E}\,. \tag{21}$$

Based on the characteristics of the numerical model of the pier mentioned above, the boundary conditions are:

$$(\sigma_r)_{r=1}=0\,, \tag{22}$$

$$(u_r)_{r=0}=0\,. \tag{23}$$

By solving Eqs. (18), (21), the coefficients A and C can be determined, and are given as follow:

$$A=0,\ C=\frac{E\alpha}{(1-\mu)}\int_0^1 T(r)rdr\,. \tag{24}$$

3 Results and discussions

3.1 Calibration of numerical model

In this study, to verify the numerical model, the cylindrical pier is simulated as per the analytical study under adiabatic heating condition. The numerical simulation results are compared with the results from the analytical solutions. The results at E2 located on the outer edge of the pier as shown in Fig. 2 (c) are selected for comparison.

Fig. 4 shows the radial temperature field of cylindrical pier as shown in Fig. 2 (c) induced by concrete

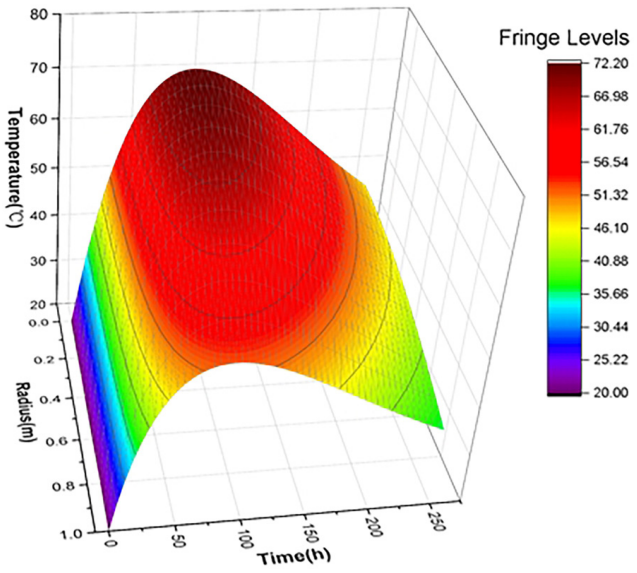

Fig. 4 Temperature field distribution of pile induced by concrete hydration heat

hydration heat. As shown, the temperature field of the pier is related to the age and location of concrete. At the initial time after pouring, the temperature of the entire pier is equal to the pouring temperature of concrete. As the age of concrete increases, the temperature of pier begins to rise, and the temperature at the center of the pier rises the fastest because there is less heat exchange between the concrete here and the outer environment. Along the radial direction of the pier, the hydration heat temperature of the concrete gradually decreases. The convection between concrete and air causes some of the hydration heat of concrete to be transferred to air.

Fig. 5 shows the stress at E2 obtained from the numerical simulation and analytical derivation. The analytical result is calculated based on the temperature field of pile induced by concrete hydration heat as shown in Fig. 4. It can be seen that the stress time histories obtained from two methods agree very well, which proves the accuracy of numerical simulation.

3.2 Influence of adiabatic temperature rise

The adiabatic temperature rise of concrete is mainly controlled by the maximum adiabatic temperature rise and the reaction rate coefficient of concrete. Fig. 6 shows the temperature time histories at E1 under different maximum adiabatic temperature rises. As shown, the peak value of temperature at the center of the pier increases with the increase of maximum adiabatic temperature rise of concrete. The temperature at the center of the pier is time-dependent. The increase of temperature at the center of the pier is caused by the heat of concrete hydration. When the value of hydration heat is less than that of the heat dissipation between the outer surface of the pier and the environment, the temperature at the center of the pier begins to decrease.

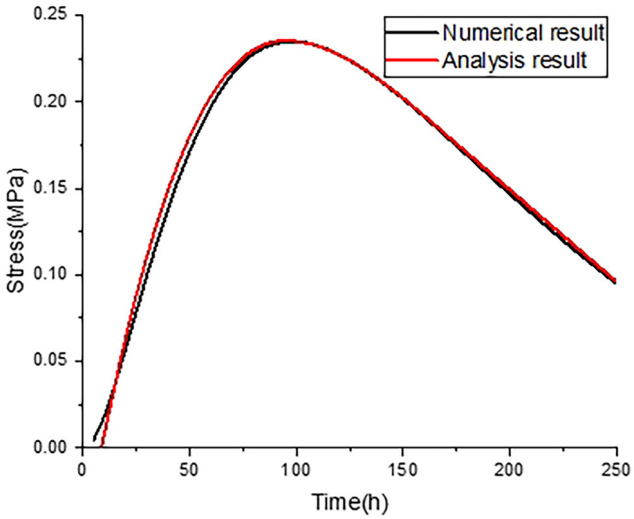

Fig. 5 Stress time histories at E2

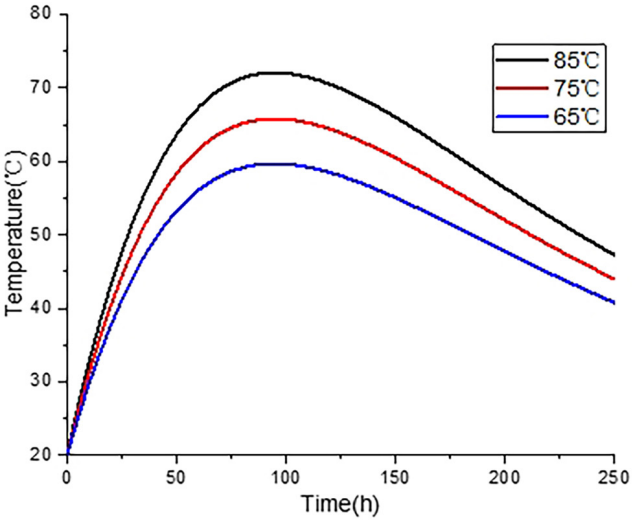

Fig. 6 Temperature time histories at E1 under different maximum adiabatic temperature rises

Fig. 7 shows the stress time histories at E2 under different maximum adiabatic temperature rises. Fig. 8 shows the stress contours of pier subjected to different maximum adiabatic temperature rises. As shown, the peak value of thermal stress at E2 is time-dependent. The peak value of thermal stress at E2 increases with the increase of maximum adiabatic temperature rise of concrete because the higher maximum adiabatic temperature rise results in a higher temperature difference between the outer boundary of the pier and the environment as shown in Fig. 8. Therefore, in order to reduce the thermal stress of massive

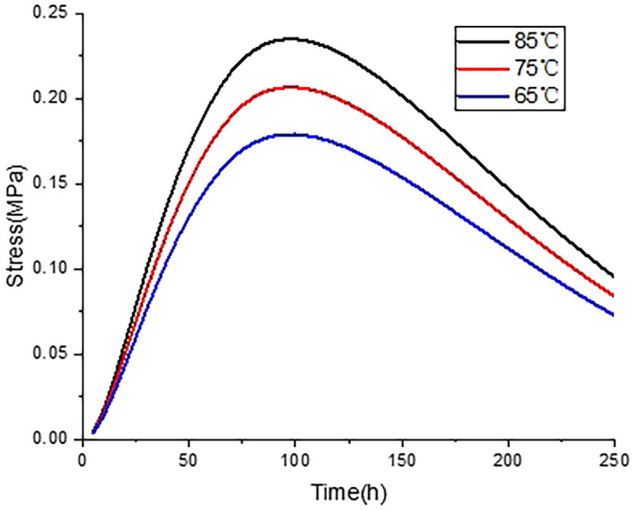

Fig. 7 Stress time histories at E2 under different maximum adiabatic temperature rises

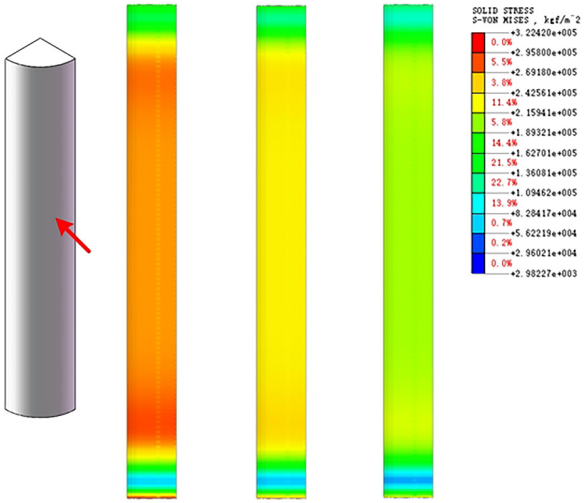

Fig. 8 Stress contours of pier under different maximum adiabatic temperature rises (a) 85 °C; (b) 75 °C; (c) 65 °C

concrete pier, the maximum adiabatic temperature rise of concrete should be reduced.

Figs. 9 and 10 show the temperature and stress time histories at E1 and E2 under different reaction rate coefficients of concrete, respectively. As illustrated, the peak value of temperature and stress increase with the increase of reaction rate coefficient, which means concrete generates more hydration heat per unit time. To reduce the thermal stress of massive concrete pier, the reaction rate coefficient of concrete should be decreased.

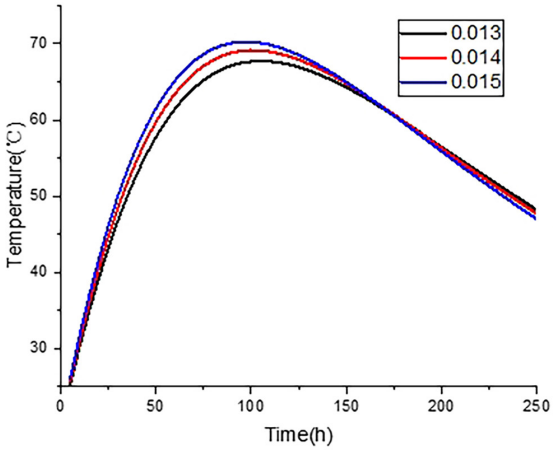

Fig. 9 Temperature time histories at E1 under different reaction rate coefficients of concrete

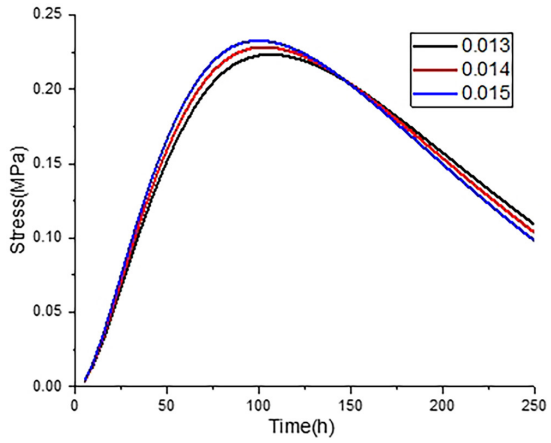

Fig. 10 Stress time histories at E2 under different reaction rate coefficients of concrete

3.3 Influence of ambient temperature

Fig. 11 shows the temperature time histories at E1 under different ambient temperatures. As shown, the temperature at the center of the pier is related to the ambient temperature, and the temperature at the center of pier increases with the increase of the ambient temperature. This is because the higher the ambient temperature, the less heat dissipation between concrete and environment, and which promotes an increase in the peak value of temperature of the pier.

Fig. 12 shows the stress time histories of pier under different ambient temperatures. As shown, during the initial stage of concrete pouring, the lower the ambient

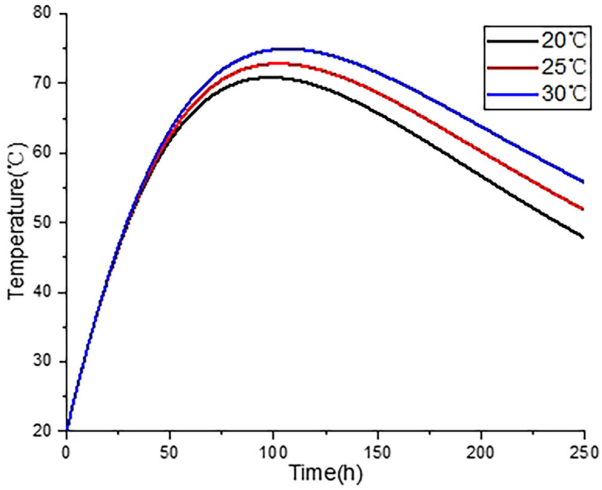

Fig. 11 Temperature time histories at E1 under different ambient temperatures

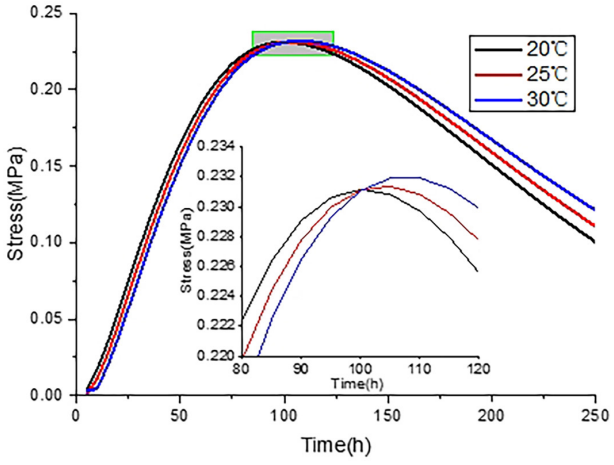

Fig. 12 Stress time histories at E2 under different ambient temperatures

temperature, the higher the thermal stress on the outer surface of the pier, which is caused by the temperature difference between the pier and the external environment. In order to reduce the stress on the surface of the pier, the temperature difference between the materials on both sides of the external surface of the pier should be reduced. The maximum value of stress at the outer surface of pier is related to the ambient temperature. The maximum stress value gets higher with higher ambient temperature because more hydration heat of concrete is contributed to rise the temperature of the pier, resulting in a higher temperature difference on both sides of the external surface of the pier. The stress on the external surface of the pier reduce rapidly when the ambient temperature is low, which is induced by the high heat flow rate between pier and air.

3.4 Influence of convection coefficient

Fig. 13 shows the temperature time histories at E1 under different convection coefficients. As shown, the temperature decreases more rapidly as the convection coefficient increases. Increasing the convection coefficient of the boundary can increase the heat dissipation of the concrete, and lead to a smaller peak temperature.

Fig. 14 shows the stress time histories of pier under different convection coefficients. As shown, the convection coefficient has a significant effect on the stress of pier. The peak value of stress at E2 reduces with the decrease of convection coefficient. This is because the smaller the convection coefficient, the less heat dissipation of the concrete, and the smaller the temperature change on the cross-section of the pier as shown in Fig. 15. Therefore, the convection coefficient around pier should be reduced to control the thermal stress of the massive concrete pier.

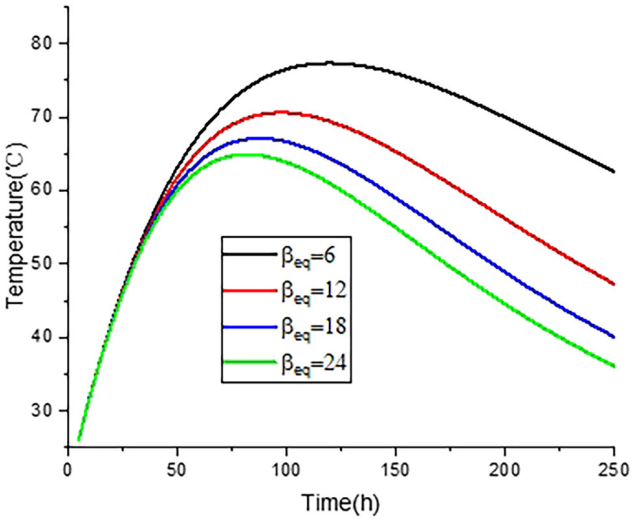

Fig. 13 Temperature time histories at E1 under different convection coefficients

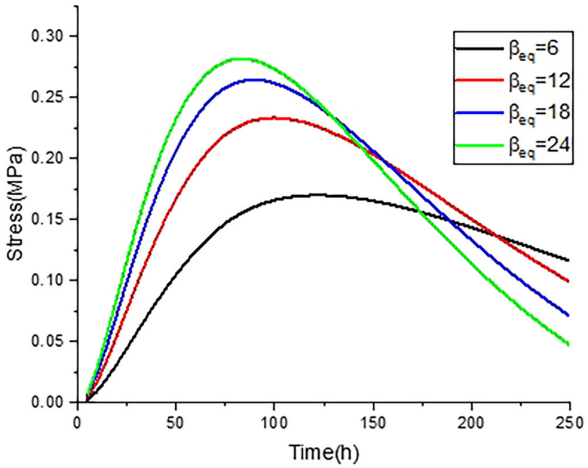

Fig. 14 Stress time histories at E2 under different convection coefficients

4 Conclusions

In this study, a 3D numerical model of massive concrete pier is established via the commercial software Midas FEA NX. The influences of adiabatic temperature rise, ambient temperature and convection coefficient on the temperature and thermal stress field of pier are studied. The main conclusions are drawn below.

1. The temperature field of the pier is related to the age and location of concrete. As the age of concrete increases, the temperature of pier begins to rise, and the temperature at the center of the pier rises the fastest because there is less heat exchange between the concrete here and the outer environment. Along the

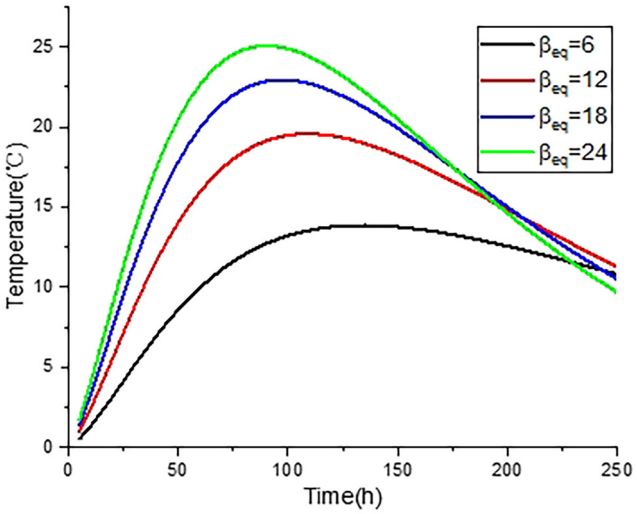

Fig. 15 Temperature difference time histories between E1 and E2 under different convection coefficients

radial direction of the pier, the hydration heat temperature of the concrete gradually decreases.

2. The peak values of temperature and stress of the pier increases with the increase of the maximum adiabatic temperature rise, the reaction rate coefficient and the ambient temperature.
3. The peak value of stress reduces with the decrease of convection coefficient because the heat dissipation of concrete reduces with the decrease of the convection coefficient.

In this study, an analytical solution for the thermal stress caused by the hydration heat of concrete piers is provided, which enables rapid calculation of thermal stress in massive concrete components. However, the theoretical model of this study is relatively simple. In the following research, the effect of pier shape on the temperature stress analysis algorithm will be studied.

Acknowledgement

The authors are grateful for the financial support from the China State Construction Engineering Corporation via CSCEC-2021-Z-30.

References

[1] Lawrence, A. "A finite element model for the prediction of thermal stresses in mass concrete", Level (PhD), University of Florida, 2009.

[2] Chu, I., Kwon, S. H., Amin, M. N., Kim, J.-K. "Estimation of temperature effects on autogenous shrinkage of concrete by a new prediction model", Construction and Building Materials, 35, pp. 171–182. https://doi.org/10.1016/j.conbuildmat.2012.03.005

[3] Klemczak, B., Batog, M., Giergiczny, Z., Żmij, A. "Complex effect of concrete composition on the thermo-mechanical behaviour of mass concrete", Materials, 11(11), 2207, 2018. https://doi.org/10.3390/ma11112207

[4] Yeon, J. H., Choi, S., Won, M. C. "In situ measurement of coefficient of thermal expansion in hardening concrete and its effect on thermal stress development", Construction and Building Materials, 38, pp. 306–315, 2013. https://doi.org/10.1016/j.conbuildmat.2012.07.111

[5] Chu, I., Lee, Y., Amin, M. N., Jang, B.-S., Kim, J.-K. "Application of a thermal stress device for the prediction of stresses due to hydration heat in mass concrete structure", Construction and Building Materials, 45, pp. 192–198, 2013. https://doi.org/10.1016/j.conbuildmat.2013.03.056

[6] Barrett, P. R., Foadian, H., James, R. J., Rashid, Y. R. "Thermal-structural analysis methods for RCC dams", In: 3rd ASCE Specialty Conference on Roller Compacted Concrete, San Diego, CA, USA, 2015, pp. 407–422. ISBN 9780872628625

[7] Emborg, M., Bernander, S. "Assessment of risk of thermal cracking in hardening concrete", Journal of Structural Engineering, 120(10), 2893–2912, 1994. https://doi.org/10.1061/(ASCE)0733-9445(1994)120:10(2893)

[8] Mansour, D. M., Ebid, A. M. "Modeling of heat transfer in massive concrete foundations using 3D-FDM", Civil Engineering Journal, 9(10), pp. 2430–2444, 2023. https://doi.org/10.28991/CEJ-2023-09-10-05

[9] Mansour, D., Ebid, A. "Predicting thermal behavior of mass concrete elements using 3D finite difference model", Asian Journal of Civil Engineering, 25(6), pp. 1601–1611, 2023. https://doi.org/10.1007/s42107-023-00864-2

[10] Zienkiewicz, O. C. "The computation of shrinkage and thermal stresses in massive structures", Ice Proceedings, 4(1), pp. 88–100, 1955. https://doi.org/10.1680/iicep.1955.11317

[11] Xie, Y., Du, W., Xu, Y., Peng, B., Qian, C. "Temperature field evolution of mass concrete: From hydration dynamics, finite element models to real concrete structure", Journal of Building Engineering, 65, 105699, 2023. https://doi.org/10.1016/j.jobe.2022.105699

[12] Zienkiewicz, O. C., Zhu, J. Z. "The superconvergent patch recovery and a posteriori error estimates. Part I.: The recovery technique", International Journal for Numerical Methods in Engineering, 33(7), pp. 1331–1364, 1992. https://doi.org/10.1002/nme.1620330702

[13] Sheng, X., Xiao, S., Zheng, W., Sun, H., Yang, Y., Ma, K. "Experimental and finite element investigations on hydration heat and early cracks in massive concrete piers", Case Studies in Construction Materials, 18, e01926, 2023. https://doi.org/10.1016/j.cscm.2023.e01926

[14] Luo, T., Wang, X., Zhuang, S. "Value-added utilization of steel slag as a hydration heat controlling material to prepare sustainable and green mass concrete, Case Studies in Construction Materials, 19, e02619, 2023. https://doi.org/10.1016/j.cscm.2023.e02619

[15] Gao, J., Chen, W., Yu, B., Fan, P., Zhao, B., Hu, J., Zhang, D., Fang, G., Peng, F. "Effect of temperature on the mechanical behaviours of a single-ply weave-reinforced shape memory polymer composite, Composites Part B: Engineering, 159, pp. 336–345, 2019. https://doi.org/10.1016/j.compositesb.2018.09.029

[16] Zhu, H., Hu, Y., Ma, R., Wang, J., Li, Q. "Concrete thermal failure criteria, test method, and mechanism: A review", Construction and Building Materials, 283, 122762, 2021. https://doi.org/10.1016/j.conbuildmat.2021.122762

[17] Tatro, S. B., Schrader, E. K. "Thermal considerations for roller-compacted concrete", aci Structural Journal, 82(2), pp. 119–128, 1985. https://doi.org/10.14359/10319

[18] Machida, N., Uehara, K. "Nonlinear thermal stress analysis of a massive concrete structure", Computers and Structures, 26(1–2), pp. 287–296, 1987. https://doi.org/10.1016/0045-7949(87)90259-8

[19] Midas China "Midas FEA NX, (V2017)", [computer program] Available at: https://product.midasit.cn/index/products-FEANX-bridge.asp [Accessed: 17 January 2015]

[20] Zhang, Z., Guo, X., Du, R. "Analysis of hydration heat-induced stresses and cracks in massive concrete walls", Journal of Hehai University, 5, pp. 12–16, 2002.

[21] Wang, X., Wang, Q., Zhou, Y., Wang, L. "Forecast on temperature field of massive concrete based on artificial neural network", Concrete 9, pp. 21–24, 2006. [online] Available at: https://cfffgc1d129f57bb244a4svn5cv9v06cxp6c9ffgfy.eds.tju.edu.cn/nzkhtml/xmlRead/trialRead.html?dbCode=CJFD&tableName=CJFDTOTAL&fileName=HLTF200609006&fileSourceType=1&invoice=Bk1VXS9INoPe3l%2b%2bJpsZMdX-%2f3JfacoBV4TlDzNYGKCV2kUgMUkrAiipcmRGz9BgED-mUng3KL%2foWA75Vk89PukOe4zkR7Cxz85xiXLkFnqlAs-b8ywLKyU%2bY12rPJIt04zErHd4DM3QDPhJou0GM%2fCf-DxRbZ6ShJhKFshYILdHqIQ%3d&appId=KNS_BASIC_PSMC [Accessed: 17 December 2024]

[22] Li, Z.-N., Zhu, H.-B., Zhao, Y., Luo, X., Xu, R.-Q. "Thermal stress analysis and crack control of assembled bridge pier", Journal of Zhejiang University (Engineering Science), 55(1), pp. 46–54, 2021. https://doi.org/10.3785/j.issn.1008-973X.2021.01.006

[23] Jiang, Z. "Construction calculation manual", China Architecture and Building Press Beijing, 2007. ISBN 978-7-112-21911-7 [online] Available at: https://www.cabplink.com/commodity-details?productCode=5737782285642 [Accessed: 17 December 2024]

[24] Do, T. A., Hoang, T. T., Bui-Tien, T., Hoang, H. V., Do, T. D., Nguyen, P. A. "Evaluation of heat of hydration, temperature evolution and thermal cracking risk in high-strength concrete at early ages", Case Studies in Thermal Engineering, 21, 100658, 2020. https://doi.org/10.1016/j.csite.2020.100658

[25] Huang, Y., Liu, G., Huang, S., Rao, R., Hu, C. "Experimental and finite element investigations on the temperature field of a massive bridge pier caused by the hydration heat of concrete", Construction and Building Materials, 192, pp. 240–252, 2018. https://doi.org/10.1016/j.conbuildmat.2018.10.128

[26] Zhang, Z., Liu, Y., Liu, J., Zhang, N. "Thermo-mechanical behavior simulation and cracking risk evaluation on steel-concrete composite girders during hydration process", Structures, 33, pp. 3912–3928, 2021. https://doi.org/10.1016/j.istruc.2021.06.101

[27] Zhu, B. "Thermal stresses and temperature control of mass concrete", Tsing Hua University Press, 2014. ISBN 9787302362579 [online] Available at: http://www.tup.tsinghua.edu.cn/booksCenter/book_05034301.html [Accessed: 17 December 2024]

[28] Xie, Y., Qian, C. "A novel numerical method for predicting the hydration heat of concrete based on thermodynamic model and finite element analysis", Materials and Design, 226(2), 111675, 2023. https://doi.org/10.1016/j.matdes.2023.111675

[29] Rosales-Vera, M. "Cartesian Graetz problem with boundary condition of the third kind: A semi-analytical solution", International Journal of Thermofluids, 14, 100146, 2022. https://doi.org/10.1016/j.ijft.2022.100146